AngioMoCo

AngioMoCo: Learning-Based Motion Correction in Cerebral Digital Subtraction Angiography

Ruisheng Su[1,6](✉), Matthijs van der Sluijs[1], Sandra Cornelissen[1], Wimvan Zwam[2], Aad van der Lugt[1], Wiro Niessen[1,3], Danny Ruijters[4], Theo van Walsum[1], and Adrian Dalca[5,6]

[1] Erasmus University Medical Center, Rotterdam, The Netherlands
r.su@erasmusmc.nl
[2] Maastricht University Medical Center, Maastricht, The Netherlands
[3] Delft University of Technology, Delft, The Netherlands
[4] Philips Healthcare, Best, The Netherlands
[5] Massachusetts Institute of Technology, Boston, USA
[6] Massachusetts General Hospital, Harvard Medical School, Boston, USA

Abstract. Cerebral X-ray digital subtraction angiography (DSA) is the standard imaging technique for visualizing blood flow and guiding endovascular treatments. The quality of DSA is often negatively impacted by body motion during acquisition, leading to decreased diagnostic value. Traditional methods address motion correction based on non-rigid registration and employ sparse key points and non-rigidity penalties to limit vessel distortion, which is time-consuming. Recent methods alleviate subtraction artifacts by predicting the subtracted frame from the corresponding unsubtracted frame, but do not explicitly compensate for motion-induced misalignment between frames. This hinders the serial evaluation of blood flow, and often causes undesired vasculature and contrast flow alterations, leading to impeded usability in clinical practice. To address these limitations, we present AngioMoCo, a learning-based framework that generates motion-compensated DSA sequences from X-ray angiography. AngioMoCo integrates contrast extraction and motion correction, enabling differentiation between patient motion and intensity changes caused by contrast flow. This strategy improves registration quality while being orders of magnitude faster than iterative elastix-based methods. We demonstrate AngioMoCo on a large national multi-center dataset (MR CLEAN Registry) of clinically acquired angiographic images through comprehensive qualitative and quantitative analyses. AngioMoCo produces high-quality motion-compensated DSA, removing while preserving contrast flow. Code is publicly available at https://github.com/RuishengSu/AngioMoCo.

Keywords: Angiography · X-Rays · Registration · Motion Artifacts

Supplementary Information The online version contains supplementary material available at https://doi.org/10.1007/978-3-031-43990-2_72.

H. Greenspan et al. (Eds.): MICCAI 2023, LNCS 14226, pp. 770–780, 2023.
https://doi.org/10.1007/978-3-031-43990-2_72

1 Introduction

Cerebral X-ray digital subtraction angiography (DSA) is a widely used imaging modality in interventional radiology for blood flow visualization and therapeutic guidance in endovascular treatments [25]. It is a 2D+T image series obtained by subtracting an initial pre-contrast image from subsequent post-contrast frames, leaving only the contrast-filled vessels visible. The injection of contrast medium and the subtraction process effectively eliminate soft tissue and bone, enabling high-resolution visualization of the vessels and the blood flow. However, this subtraction technique assumes the absence of motion between frames during exposure. In clinical practice, this premise is often violated. Involuntary motions, caused by swallowing, coughing, stroke, or endovascular procedures, are nearly inevitable. Body motion results in undesired artifacts in subtracted images, leading to decreased image quality and impaired interpretability of DSA (Fig. 1).

Over the last three decades, various motion correction techniques have been proposed to mitigate the impact of body motion retrospectively [18]. Registration algorithms typically employ template matching with corresponding control points or landmarks to align images [3,4,6–10,16,17,19,22,26–28]. These algorithms rely on features based on vessels [8], edges [9,17,19,28], corners [30], textures [20], temporal correspondence [3], and non-uniform grids [27]. To capture both local and global transformations, multi-resolution search [21,31], block

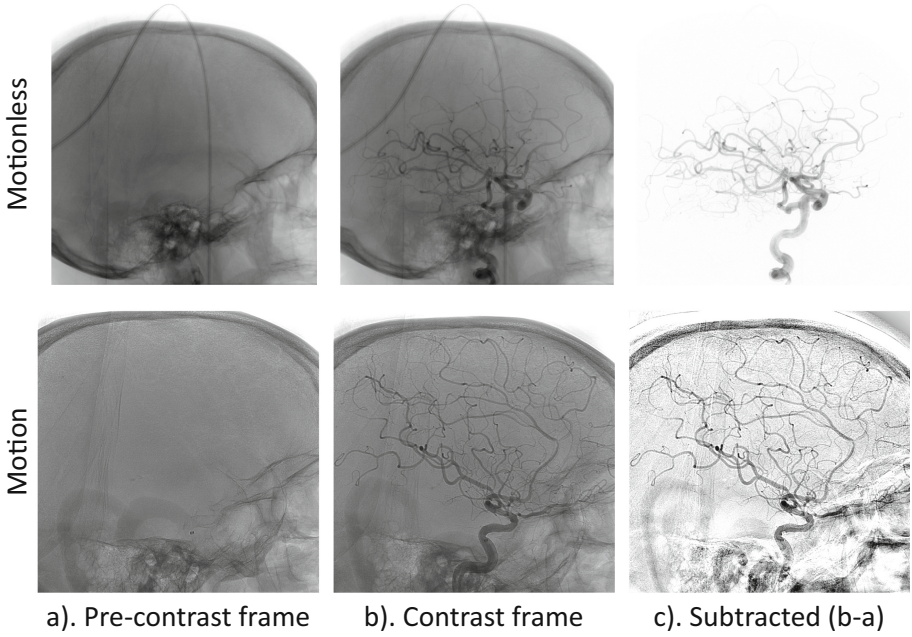

Fig. 1. Illustration of motion artifacts in DSA: a) the pre-contrast frame; b) a subsequent post-contrast frame; c) subtracted frame (b-a).

matching [9], and iterative estimations [20,30] have been proposed. To limit undesirable vessel distortions, sparse key points [19] and non-rigidity penalties [26] have been used. Although these methods are effective in motion compensation, they require time-consuming iterative computation for each frame, limiting their clinical applicability.

Recent generative models, such as pix2pix [13], have been adapted to address subtraction artifacts without registration [11,12,29]. These models leverage deep learning techniques to predict a subtraction image from an input post-contrast image by discerning foreground contrast from the body background, resulting in reduced artifacts. However, these models do not explicitly compensate for motion-induced misalignment between frames. More importantly, they may cause hallucinations or modification of contrast and vessels, and lack interpretability as there is no subtraction. Consequently, these shortcomings hinder the serial evaluation of blood flow and impede the diagnostic utility of DSA.

To overcome these limitations, we introduce AngioMoCo, a fast learning-based motion correction method for DSA that avoids severe contrast distortion. We employ a supervised CNN module that distinguishes between motion displacement and contrast intensity change. The output contrast-removed image and the pre-contrast image are then input to a subsequent self-supervised learning-based registration model for deformable registration, where a deformation regularization loss limits the local irregularity. By excluding contrast enhancements from the deformation learning processing, AngioMoCo avoids undesired distortion of the vessels. This results in trustworthy visualization of continuous blood flow and promises to assist in automated analysis of flow-based biomarkers relevant to endovascular treatments.

Overall, classical non-rigid registration methods use various regularization strategies to limit vessel distortion, but are prohibitively time-consuming. Recent learning-based methods are fast, but do not explicitly model the motion between frames, and as a result can negatively distort the very clinical information we aim to highlight. We build on the strengths of both directions while avoiding their limitations. Specifically, we propose a novel learning-based strategy that is significantly faster than traditional non-rigid registration methods. AngioMoCo not only removes subtraction artifacts on each frame but does so by explicitly compensating for motion between frames, which is not available in existing image-to-image models. We demonstrate that AngioMoCo achieves high-quality registration while avoiding undesirable contrast reduction or vessel erasure.

2 Method

2.1 Model

Figure 2 outlines the AngioMoCo framework for motion correction and subtraction in angiographic images, comprising three main modules: contrast extraction, deformable registration, and spatial-transformed subtraction. Let $\mathcal{X} = \{x_t\}_{t=0}^{T}$ be the 2D+T DSA series of a patient, where x_0 is the pre-contrast frame and $\{x_t\}_{t=1}^{T}$ are the post-contrast frames.

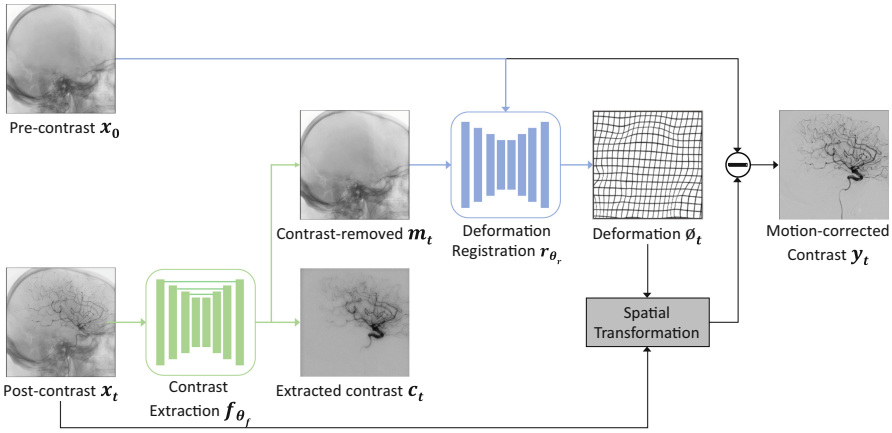

Fig. 2. Overview. The proposed framework takes a pre-contrast image x_0 and a post-contrast image x_t as input. The contrast extraction module $f_{\theta_f}(\cdot)$ splits x_t into contrast c_t and contrast-removed m_t. Next, m_t and x_0 are registered using network $r_{\theta_r}(\cdot,\cdot)$, which outputs a deformation field ϕ_t. Subsequently, ϕ_t is applied to the post-contrast image x_t to obtain the final output subtracted image y_t, which corrects misalignment between frames.

We define a contrast extraction module $f_{\theta_f}(x_t) = c_t$ with parameters θ_f that takes as input a post-contrast frame x_t. This function separates x_t into a contrast image c_t and a contrast-removed image m_t where $m_t = x_t - c_t$. The values in c_t are within $[-1,\ 0]$ as the injected contrast medium can only lead to a decrease in pixel intensity relative to the input image with an intensity range of $[0,\ 1]$. The contrast extraction module aims to reduce contrast discrepancies between the pre- and post-contrast frames. Such image-to-image modules can lead to hallucination and may not fully capture distal vessels, relatively less contrasted vessels, and vessels behind bone structures. Therefore, in AngioMoCo, we only employ this module to enable easier registration of the frame x_t to the pre-contrast x_0 using the intermediate contrast-extracted m_t image.

We define a registration function $r_{\theta_r}(x_0, m_t) = \phi_t$ with parameters θ_r to estimate the deformation ϕ_t. We obtain the motionless subtraction angiography y_t by subtracting the pre-contrast frame x_0 from the warped post-contrast frame w_t: $y_t = w_t - x_0 = x_t \circ \phi_t - x_0$, where $\circ$ defines a spatial warp.

2.2 Training

We train the contrast extraction $f_{\theta_f}(\cdot)$ and deformable registration $r_{\theta_r}(\cdot,\cdot)$ modules separately. The contrast extraction module is trained on a motionless subset of data with an MSE loss between the ground truth contrast, estimated via subtraction between post- and pre-contrast frames $(x_t - x_0)$, and the predicted c_t:

$$\mathcal{L}_{\text{ext}}(\theta_r; x_t) = \mathcal{L}_{\text{MSE}}(x_t - x_0, f_{\theta_f}(x_t)). \tag{1}$$

We train the deformable registration module on a motion subset, with the pre-trained contrast extraction module frozen, using a loss function that combines an MSE loss between m_t and x_0 and a smoothness loss $\mathcal{L}_{\text{smooth}}$, weighted by λ:

$$\mathcal{L}_{\text{reg}}(\theta_f; x_0, m_t \circ \phi_t) = (1-\lambda)\mathcal{L}_{\text{MSE}}(x_0, m_t \circ \phi_t) + \lambda \mathcal{L}_{\text{smooth}}(\phi_t), \tag{2}$$

where $\mathcal{L}_{\text{smooth}}$ is the mean squared horizontal and vertical gradients of displacement u_t in deformation field ϕ_t, that enforces spatial smoothness of deformation:

$$\mathcal{L}_{\text{smooth}}(\phi_t) = \|\nabla u_t\|^2. \tag{3}$$

2.3 Architecture

We design the contrast extraction module $f_{\theta_f}(\cdot,\cdot)$ using a U-Net architecture, which includes a contracting path (encoder) and an expanding path (decoder) connected by skip connections. The encoder stage comprises eight convolutional and max-pooling layers with the number of channels being 8, 16, 32, 64, 128, 256, 512, and 512 respectively. The convolutions operate with a 3×3 kernel size and a stride of 2. Similarly, the decoding path employs eight upsampling, 3×3 convolution, and concatenation operations with 32 feature maps per layer to restore the spatial dimension up to the input size. Each convolution is accompanied by an instance normalization and a LeakyReLU activation layer. We also use three additional 3×3 convolutions. The final convolution employs a negative sigmoid activation, confining the output pixel intensity to $[-1, 0]$.

We employ a deformable registration module $r_{\theta_r}(\cdot,\cdot)$ based on VoxelMorph to learn motion correction in DSA [2]. We add instance normalization between the convolution layers of the encoder and decoder. We utilize this deformable registration module to predict bi-directional dense deformation fields using diffeomorphism that allows to spatially transform either pre- or post-contrast frames.

3 Experiments

We assess AngioMoCo in terms of vessel contrast preservation, artifact removal, and computation efficiency compared to existing approaches.

3.1 Experimental Setup

Data. We identified 272 patients with unsubtracted cerebral angiographic images available from MR CLEAN registry [14], an ongoing prospective observational multi-center registry of patients with acute ischemic stroke who underwent endovascular thrombectomy (EVT). This comprised 788 angiographic series, consisting of 16,641 frames in total, acquired between attempts of thrombus retrieval. The DSA series were acquired using various imaging systems, including Philips, GE, and Siemens, and had a size of 1024×1024 pixels. The series had varying lengths, ranging from 10 to 50 frames, and temporal resolutions between 0.5 and 4 frames per second (fps). We performed image resizing to 512×512

pixels and min-max intensity normalization to obtain intensity values within the range of $[0, 1]$. To ensure the coherency of the intensity along the series, the maximum intensity is calculated on the series level based on the stored bits in the DICOM header.

Based on visual assessment, we categorized the dataset into two subsets: motionless and motion. We use the motionless subset, consisting of 107 series (1933 frames) from 21 patients, for pre-training the contrast extraction module. The motion subset, which contains 681 series (14708 frames) from 251 patients, is used for overall training and evaluation. We split data on the patient level independently on the motionless and motion subsets, with a ratio of 50%, 20%, and 30% for training, validation, and testing, respectively.

Baselines. We compare AngioMoCo with two widely used image registration approaches, elastix-based affine registration and VoxelMorph [1,2], and an image-to-image approach employing a U-Net [24] architecture. We followed the implementation of [2] for VoxelMorph with deformation regularization $\lambda = 0.01$. For the U-Net, we employed the same architecture as the contrast extraction module $f_{\theta_f}(\cdot, \cdot)$ with the same preprocessing and augmentations. We trained the U-Net using the motionless subset and used mean squared error (MSE) as the optimizing objective. We implemented the methods using Python 3.10.6 and PyTorch [23].

Training Details. We use an NVIDIA 2080 Ti GPU (11 GB), the Adam optimizer [15] and the ReduceLROnPlateau scheduler with an initial learning rate of 0.001, a patience of 300 epochs, and a decay of 0.1. We set the batch size to 8 and applied early stopping with a patience of 500 epochs. We selected these optimization parameters based on validation performance using a grid search. We applied data augmentations using Albumentations [5], including *HorizontalFlip*, *ShiftScaleRotate*, and *RandomSizedCrop*, each with a probability of 0.5.

Evaluation. We carry out both qualitative and quantitative analyses on the hold-out test set of the motion subset. A key challenge is to minimize motion and subtraction artifacts while retaining clinically important features. We use mean squared intensity (MSI) as a proxy to quantify the preservation of contrast intensity within vessels and the ability of motion correction outside vessels. As ground truth deformations are not available for image sequences with motion, we manually segment the blood vessels in post-contrast frames (Supplemental Fig. 6), and use the resulting masks to quantify MSI inside and outside blood vessels. We used paired t-tests for statistical significance.

3.2 Results

Quantitative Analysis. The optimal outcome is represented by the top left corner of Fig. 3, indicating high vessel contrast preservation and complete artifact removal (Supplemental Table 1). Compared to elastix affine registration,

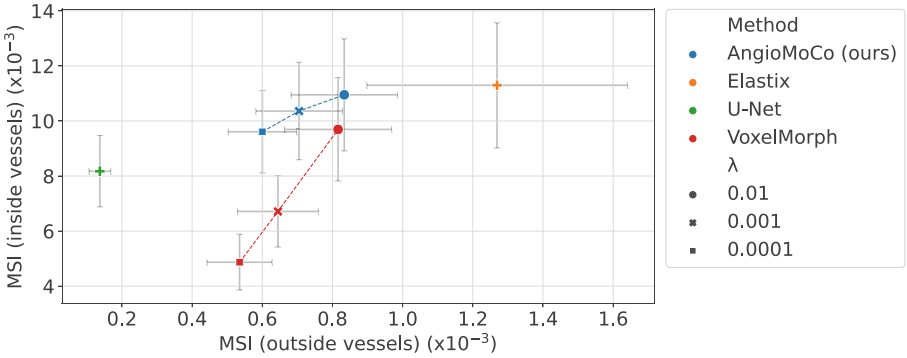

Fig. 3. Mean squared intensity (MSI) on the test set. Better methods will preserve the MSI (i.e., vessel contrast) inside vessels (↑, y-axis) while minimizing the MSI (i.e., artifacts) outside vessels (←, x-axis), moving towards the top left of the graph.

AngioMoCo($\lambda = 0.001$) achieves similar vessel preservation (P = 0.2), while substantially decreasing the MSI outside vessels (by about half). Compared to VoxelMorph, AngioMoCo demonstrates substantial improvement, with higher vessel preservation and better (more to the left) artifact removal. While the image-to-image U-Net yields the lowest MSI outside vessels, it sacrifices a substantial amount (30%) of contrast inside vessels, harming the precise clinical signal we are interested in.

Qualitative Analysis. Figure 4 presents visual comparisons of the methods through three representative examples. The image-to-image U-Net generates images with fewer motion artifacts than other methods, but it often fails to capture vessel contrast behind bone structures (Row 1), distal vessels (Row 1), and loses high-frequency spatial features, leading to blurry images (Row 2). These errors can have substantial negative effects on downstream clinical applications. VoxelMorph operates on pre- and post-contrast images, which can cause considerable modifications in the vessel contrast flow. For example, the motion-corrected image of VoxelMorph in Row 3 has lighter vessel contrast than its counterparts. In contrast, AngioMoCo overcomes these limitations of U-Net and VoxelMorph by learning to disentangle contrast flow from motion.

Runtime. Compared to iterative registration methods, deep-learning-based registration methods, including AngioMoCo, require orders of magnitude less time. For example, AngioMoCo takes less than a second to process a series on GPU, while iterative registration methods are mostly implemented on CPU where they require minutes.

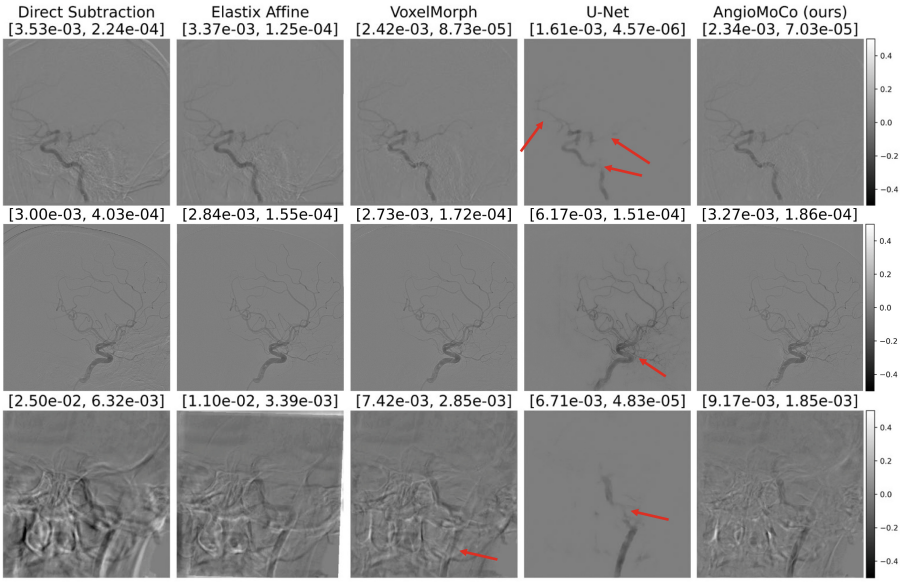

Fig. 4. Representative visual comparisons. We report MSI values inside (left) and outside (right) vessels in brackets. Red arrows point to undesired vessel contrast erasure or modifications. AngioMoCo achieves better background artifact removal and vessel enhancement than other methods. The UNet achieves excellent artifact removal, but it comes at the cost of severe damage to the vessels of interest, making it clinically less useful.

4 Discussion

We find that AngioMoCo achieves high-quality motion correction in DSA, while preserving vessel details, which is of critical clinical importance. While the image-to-image U-Net resulted in fewer artifacts, it substantially degrades the vessel contrast, harming its usability in clinical usefulness.

These results suggest that AngioMoCo is clinically relevant for endovascular applications, enhancing the utility of DSA in diagnosis and treatment planning. The tool can extract contrast flow while outputting smooth bi-directional deformation fields that provide interpretability. Unlike image-to-image models, the contrast flow visualization is driven by motion-compensation of the post-contrast frames to the pre-contrast image, and hence avoids undesirable hallucinations and modifications of vessel contrast.

We also examined the end-to-end training strategy of AngioMoCo, which did not yield superior results to VoxelMorph or the modularly trained AngioMoCo (Supplemental Fig. 5). To further enhance registration accuracy, future research may explore the integration of 3D spatio-temporal CNN and the utilization of vessel masks as auxiliary supervision.

5 Conclusion

We have presented AngioMoCo, a deep learning-based strategy towards motion-free digital subtraction angiography. The approach leverages a contrast extraction module to disentangle contrast flow from body motion and a deformable registration module to concentrate on motion-induced deformations. The experimental results on a large clinical dataset demonstrate that AngioMoCo outperforms iterative affine registration, learning-based VoxelMorph, and image-to-image U-Net. Overall, AngioMoCo achieves high registration accuracy while preserving vascular features, improving the quality and clinical utility of DSA for diagnosis and treatment planning in endovascular procedures.

Acknowledgment. This work is done during a visit at MGH. The visit was made possible in part by the Academy Van Leersum grant of the Academy Medical Sciences Fund of the Royal Netherlands Academy of Arts & Sciences (KNAW).

References

1. Balakrishnan, G., Zhao, A., Sabuncu, M.R., Guttag, J., Dalca, A.V.: An unsupervised learning model for deformable medical image registration. In: Proceedings of the IEEE Conference on Computer Vision and Pattern Recognition, pp. 9252–9260 (2018)
2. Balakrishnan, G., Zhao, A., Sabuncu, M.R., Guttag, J., Dalca, A.V.: VoxelMorph: a learning framework for deformable medical image registration. IEEE Trans. Med. Imaging **38**(8), 1788–1800 (2019)
3. Bentoutou, Y., Taleb, N.: A 3-D space-time motion detection for an invariant image registration approach in digital subtraction angiography. Comput. Vis. Image Underst. **97**(1), 30–50 (2005)
4. Bentoutou, Y., Taleb, N., El Mezouar, M.C., Taleb, M., Jetto, L.: An invariant approach for image registration in digital subtraction angiography. Pattern Recogn. **35**(12), 2853–2865 (2002)
5. Buslaev, A., Iglovikov, V.I., Khvedchenya, E., Parinov, A., Druzhinin, M., Kalinin, A.A.: Albumentations: fast and flexible image augmentations. Information **11**(2), 125 (2020)
6. Buzug, T.M., Weese, J.: Image registration for DSA quality enhancement. Comput. Med. Imaging Graph. **22**(2), 103–113 (1998)
7. Buzug, T.M., Weese, J., Fassnacht, C., Lorenz, C.: Using an entropy similarity measure to enhance the quality of DSA images with an algorithm based on template matching. In: Höhne, K.H., Kikinis, R. (eds.) Visualization in Biomedical Computing: 4th International Conference, VBC 1996 Hamburg, Germamy, 22–25 September 1996, Proceedings, pp. 235–240. Springer, Cham (2006). https://doi.org/10.1007/BFb0046959
8. Cao, Z., Liu, X., Peng, B., Moon, Y.S.: DSA image registration based on multiscale Gabor filters and mutual information. In: 2005 IEEE International Conference on Information Acquisition, pp. 6-pp. IEEE (2005)
9. Chu, Y., Bai, N., Ji, Z., Chen, S., Mou, X.: Registration for DSA image using triangle grid and spatial transformation based on stretching. In: 2006 8th international Conference on Signal Processing, vol. 2. IEEE (2006)

10. Cox, G.S., de Jager, G.: Automatic registration of temporal image pairs for digital subtraction angiography. In: Medical Imaging 1994: Image Processing, vol. 2167, pp. 188–199. SPIE (1994)
11. Crabb, B.T., et al.: Deep learning subtraction angiography: improved generalizability with transfer learning. J. Vasc. Intervent. Radiol. **34**, 409-419.e2 (2022)
12. Gao, Y., et al.: Deep learning-based digital subtraction angiography image generation. Int. J. Comput. Assist. Radiol. Surg. **14**, 1775–1784 (2019)
13. Isola, P., Zhu, J.Y., Zhou, T., Efros, A.A.: Image-to-image translation with conditional adversarial networks. In: Proceedings of the IEEE Conference on Computer Vision and Pattern Recognition, pp. 1125–1134 (2017)
14. Jansen, I.G., Mulder, M.J., Goldhoorn, R.J.B.: Endovascular treatment for acute ischaemic stroke in routine clinical practice: prospective, observational cohort study (MR CLEAN Registry). BMJ **360**, k949 (2018)
15. Kingma, D.P., Ba, J.: Adam: a method for stochastic optimization. arXiv preprint arXiv:1412.6980 (2014)
16. Liu, B., Zhao, Q., Dong, J., Jia, X., Yue, Z.: A stretching transform-based automatic nonrigid registration system for cerebrovascular digital subtraction angiography images. Int. J. Imaging Syst. Technol. **23**(2), 171–187 (2013)
17. Meijering, E.H., et al.: Reduction of patient motion artifacts in digital subtraction angiography: evaluation of a fast and fully automatic technique. Radiology **219**(1), 288–293 (2001)
18. Meijering, E.H., Niessen, W.J., Viegever, M.: Retrospective motion correction in digital subtraction angiography: a review. IEEE Trans. Med. Imaging **18**(1), 2–21 (1999)
19. Meijering, E.H., Zuiderveld, K.J., Viergever, M.A.: Image registration for digital subtraction angiography. Int. J. Comput. Vision **31**, 227–246 (1999)
20. Nejati, M., Amirfattahi, R., Sadri, S.: A fast image registration algorithm for digital subtraction angiography. In: 2010 17th Iranian Conference of Biomedical Engineering (ICBME), pp. 1–4. IEEE (2010)
21. Nejati, M., Pourghassem, H.: Multiresolution image registration in digital X-ray angiography with intensity variation modeling. J. Med. Syst. **38**, 1–10 (2014)
22. Nejati, M., Sadri, S., Amirfattahi, R.: Nonrigid image registration in digital subtraction angiography using multilevel B-spline. BioMed Res. Int. **2013**, 236315 (2013)
23. Paszke, A., et al.: PyTorch: an imperative style, high-performance deep learning library. In: Advances in Neural Information Processing Systems, pp. 8026–8037 (2019)
24. Ronneberger, O., Fischer, P., Brox, T.: U-Net: convolutional networks for biomedical image segmentation. In: Navab, N., Hornegger, J., Wells, W.M., Frangi, A.F. (eds.) MICCAI 2015, Part III. LNCS, vol. 9351, pp. 234–241. Springer, Cham (2015). https://doi.org/10.1007/978-3-319-24574-4_28
25. Shaban, S., et al.: Digital subtraction angiography in cerebrovascular disease: current practice and perspectives on diagnosis, acute treatment and prognosis. Acta Neurologica Belgica **122**(3), 763–780 (2021)
26. Staring, M., Klein, S., Pluim, J.P.: A rigidity penalty term for nonrigid registration. Med. Phys. **34**(11), 4098–4108 (2007)
27. Sundarapandian, M., Kalpathi, R., Manason, V.D.: DSA image registration using non-uniform MRF model and pivotal control points. Comput. Med. Imaging Graph. **37**(4), 323–336 (2013)
28. Taleb, N., Jetto, L.: Image registration for applications in digital subtraction angiography. Control. Eng. Pract. **6**(2), 227–238 (1998)

29. Ueda, D., et al.: Deep learning-based angiogram generation model for cerebral angiography without misregistration artifacts. Radiology **299**(3), 675–681 (2021)
30. Wang, J., Zhang, J.: An iterative refinement DSA image registration algorithm using structural image quality measure. In: 2009 Fifth International Conference on Intelligent Information Hiding and Multimedia Signal Processing, pp. 973–976. IEEE (2009)
31. Yang, J., Wang, Y., Tang, S., Zhou, S., Liu, Y., Chen, W.: Multiresolution elastic registration of X-ray angiography images using thin-plate spline. IEEE Trans. Nucl. Sci. **54**(1), 152–166 (2007)